J Electroceram (2011) 27:197–202
DOI 10.1007/s10832-011-9665-4

# Fabrication of $0.655Pb(Mg_{1/3}Nb_{2/3})O_3$-$0.345PbTiO_3$ functionally graded piezoelectric actuator by tape-casting

**Kongjun Zhu · Hui Wang · Jinhao Qiu · Jun Luo · Hongli Ji**

Received: 5 May 2011 / Accepted: 8 November 2011 / Published online: 22 November 2011


**Abstract** A $0.655Pb(Mg_{1/3}Nb_{2/3})O_3$-$0.345PbTiO_3$ (PMN-0.345PT) functionally graded (FG) piezoelectric actuator was fabricated by tape-casting. The effects of sintering temperature on the physical and electrical properties of the PMN-PT ceramics were initially investigated. High dielectric and piezoelectric properties of $d_{33}$=700pC/N, $k_p$=0.61, $\varepsilon_r$=4.77×103, tanδ=0.014, $P_r$=30.68 μC/cm$^2$ were obtained for the specimens sintered at 1200°C. Compared with the traditional solid-state reaction, the properties of the ceramics were significantly enhanced by tape-casting. The new FG piezoelectric actuator consisted of four layers, and the variation of changes in their $d_{33}$ and $\varepsilon_r$ were graded opposite the thickness direction. The relationship between displacement and voltage for the actuator was also determined, with the results showing that it was linear. The driving displacement of the free end of the actuator reached 430.668 μm.

**Keywords** Shaping · Piezoelectric properties · Perovskite · Actuator

## 1 Introduction

$Pb(Mg_{1/3}Nb_{2/3})O_3$-$PbTiO_3$ (PMN-PT) is a solid solution formed by a typical relaxor ferroelectric (PMN) and a normal ferroelectric (PT). The solution displays outstanding electrical and electromechanical properties, such as high relative permittivity, a broad maximum in dielectric constant $\varepsilon_r$, large electrostrictivity, low thermal expansion, and excellent voltage stability [1–3]. These properties have resulted in significant attention being paid to PMN-PT piezoelectric ceramics, both from fundamental and applied aspects. Applications of such ceramics include electrostrictive actuators [4, 5], multilayer capacitors [6], and piezoelectric actuators [7].

Traditional unimorph and bimorph piezoelectrics are widely used for actuator applications. These actuators are manufactured by bonding one or two piezoelectric layers to a metal shim layer, where the stress concentration and structural weakness at the bonding interface primarily cause the breakdown of the unimorph and bimorph actuators in cyclic actuation [8]. Qiu et al. [9–11] proposed a new type of functionally graded (FG) piezoelectric actuator.

In order to generate a bending deformation, it is required that the piezoelectric material on opposite sides of the actuator generates different in-plane strains under a given electric field in the thickness direction of the actuator. When the distribution of in-plane strain is linear in the thickness direction, a natural bending deformation can be produced without internal stress. In the practical manufacturing, continuous distribution of material composition is difficult, and instead, a multilayer structure is used. The stress distribution in the actuator depends on the thickness ratio of the layers, but for manufacturing convenience, the thicknesses of the four layers were set to be equal. The intermediate layers have intermediate values of material properties. Due to the gradation of material properties, the layers will generate a graded distribution of in-plane strain when

K. Zhu (✉) · H. Wang · J. Qiu · J. Luo · H. Ji
State Key Laboratory of Mechanics and Control of Mechanical Structures, Nanjing University of Aeronautics and Astronautics, Nanjing 210016, People's Republic of China
e-mail: kjzhu@nuaa.edu.cn

K. Zhu
State Key Laboratory of Digital Manufacturing Equipment and Technology of China, Huazhong University of Science and Technology,
Wuhan 430074, People's Republic of China

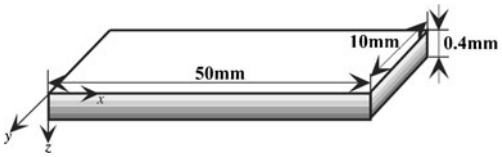


**Fig. 1** Shape and size of designed FG actuator

they are considered separately. Since all the layers are integrated in a single element, a bending deformation is generated with relatively small internal stress [11].

The layer to generate high strain has large piezoelectric constants but small dielectric constants. In contrast, the low-strain layer has small piezoelectric constants but large dielectric constants. To obtain large bending deflection, the combination of a high-strain piezoelectric material with large piezoelectric constants but small dielectric constant and a low-strain piezoelectric material with small piezoelectric constants but large dielectric constant is required. The large dielectric constant can reduce the voltage loss in the low-strain piezoelectric material [11]. In this study, four material compositions were selected from the PMN–PT family and used as the materials of the four layers in the new FG piezoelectric actuator. The compositions of the four materials are A, $0.655Pb(Mg_{1/3}Nb_{2/3})O_3$-$0.345PbTiO_3$; B, $0.850Pb(Mg_{1/3}Nb_{2/3})O_3$-$0.150PbTiO_3$; C, $0.900Pb(Mg_{1/3}Nb_{2/3})O_3$-$0.100PbTiO_3$; D, $0.920Pb(Mg_{1/3}Nb_{2/3})O_3$-$0.080PbTiO_3$, and their properties are shown in Table 2. Material A has the largest piezoelectric constant $d_{33}$ but the small dielectric constant $\varepsilon_r$. Material D has the smallest $d_{33}$ but largest $\varepsilon_r$. The four materials were laminated in the order of A–B–C–D.

Since the durability was evaluated in a vibration test, beam-shaped actuators were more suitable. The size of the FG actuator was 10 mm×50 mm×0.4 mm as shown in Fig. 1.

Tape-casting is a well-developed technique for fabricating thin film ceramic materials [12, 13]. This technique is widely used in the electronics industry for capacitors, piezoelectric and electrostrictive devices, fuel cells, catalytic substrates, and multilayer ceramic capacitors [14–19].

In the present study, a PMN-0.345PT ceramic was fabricated, and its microstructures and properties at various sintering temperatures were investigated. The properties of PMN-0.345PT ceramics prepared by both tape-casting and the traditional process were also compared. Three other materials with different compositions were selected from the PMN-PT family and used as materials for the four layers in a new FG piezoelectric actuator. The electrical properties of the fabricated actuator were also measured.

## 2 Experimental

Oxide powders of PbO (99%), $Nb_2O_5$ (99.5%), $ZrO_2$ (99%), and MgO (98.5%) were used as raw materials. Excess PbO (0.5 mol%) was added to compensate for lead loss during sintering. The raw materials were mixed by ball milling according to the material compositions at an appropriate weight percentage. The mixtures were dried in an oven and pre-calcined in a closed alumina crucible at 925°C for 4 h. Finally, the massive pre-calcined powders were crushed by hand. Two-stage ball milling was performed during slurry adjustment.

For the traditional process, 3 wt% of polyvinyl alcohol (PVA) binder was added. Discs with a diameter of 15 mm were prepared by uniaxial pressing at a presure of 250 MPa.

For the tape-casting process, at the first stage, agglomerates of pre-calcined powders were milled with a solvent and a dispersant. The second stage involved mixing and homogenization, where a plasticizer and a binder were added into the solvent/ceramic slurries. A mixed solvent (70% of methyl ethyl ketone and 30% ethanol) was used. Polyvinyl butyral, dibutyl phthalate, and corn oil were used as the binder, the plasticizer, and the dispersant, respectively. For 100 g of pre-calcined powders, the binder, plasticizer, and dispersant weights were 5, 2.5, and 0.7 g, respectively. Both stages of mixing were performed by ball milling for 8–18 h. The solvent in the slurry was evaporated, and the slurry viscosity was finally adjusted by stirring in a vacuum. Green sheets were fabricated by the tape-casting process.

Disc-shaped PMN-PT ceramic samples were obtained by punching from the green sheets. For the new FG actuator, four-composition sheets were piled up in a given order,

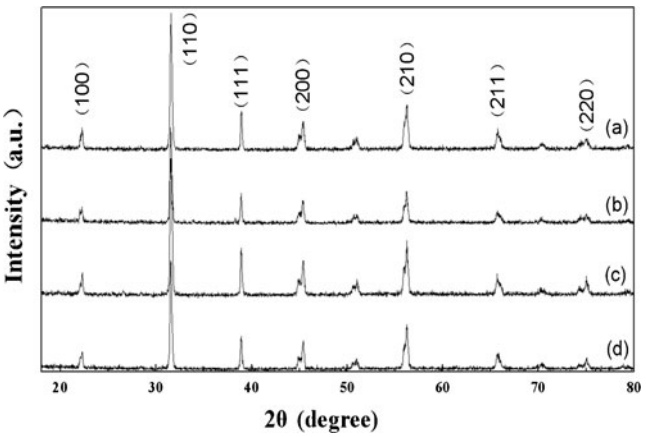


**Fig. 2** The XRD patterns of the PMN-PT ceramic sintered at various temperatures. (**a**) 1150, (**b**) 1175, (**c**) 1200, and (**d**) 1225°C

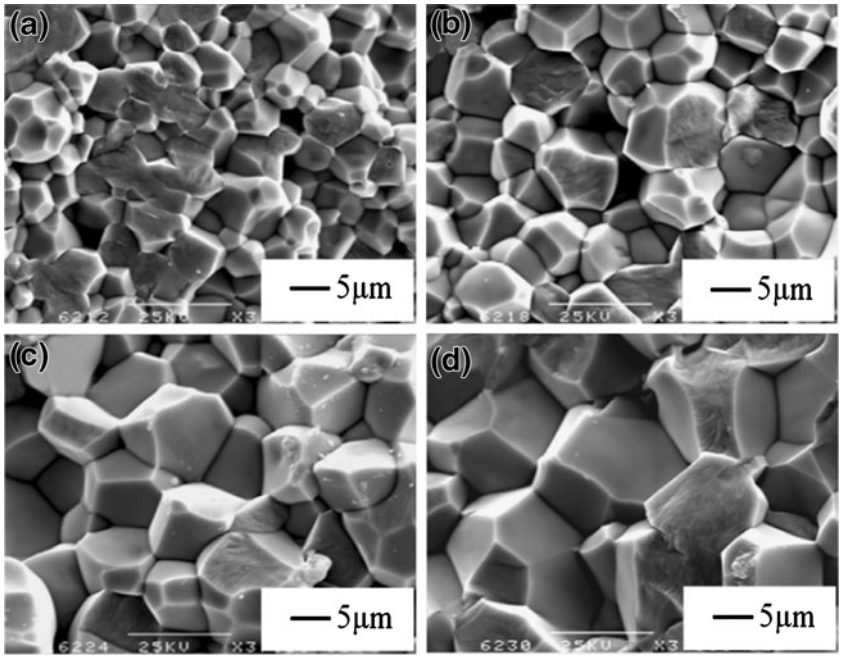


**Fig. 3** The microstructure of the cross-section of the ceramics at various temperatures (**a**) 1150, (**b**) 1175, (**c**) 1200, and (**d**) 1225°C

pressed together with heating, and then punched to the designated size. To eliminate additives in the green sheets, all fabricated ceramics were heated to 800°C in an electric furnace.

All samples were sintered at 1150, 1175, 1200, and 1225°C in a PbO-excess atmosphere. After grinding, polishing, and coating, the sintered ceramics were polarized in an oil bath at 80°C for 20 min at 2.5 KV/mm. The specimens were aged for 24 h after poling before measurements were obtained.

The perovskite-phase formation of the sintered specimens was determined by X-ray diffraction (XRD, BrukerD8 Advance, Germany) with Cu K$\alpha$ radiation ($\lambda$=0.15418 nm) at 40 kV and 40 mA using continuous scan mode. The microstructures of the sintered materials were observed using scanning electron microscopy (SEM, JEOL JSM-6300, Japan) at an accelerating voltage of 20 kV. The piezoelectric constant $d_{33}$ was measured by a piezo-$d_{33}$ meter (ZJ-3A, Institute of Acoustics Academic Sinica, Beijing, China). The $k_p$, $\varepsilon_r$, and tan $\delta$ were determined using an impedance analyzer (HP 4294A, Agilent, America) according to IEEE Standards. The polarization versus electric field (P–E) hysteresis loops of the ceramics were measured using a

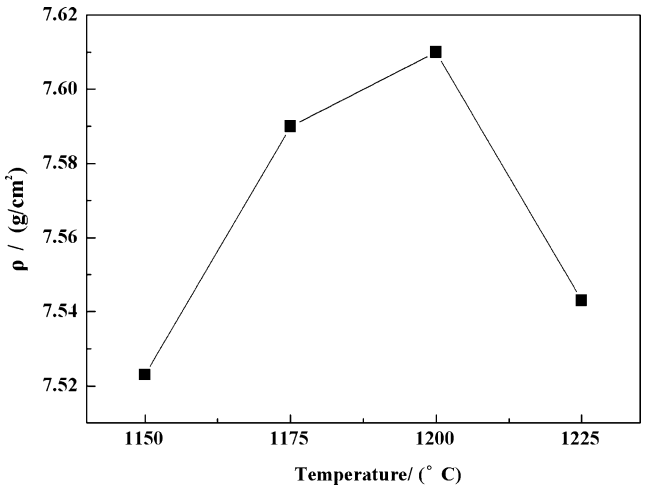


**Fig. 4** The densities of the ceramics sintered at various temperatures

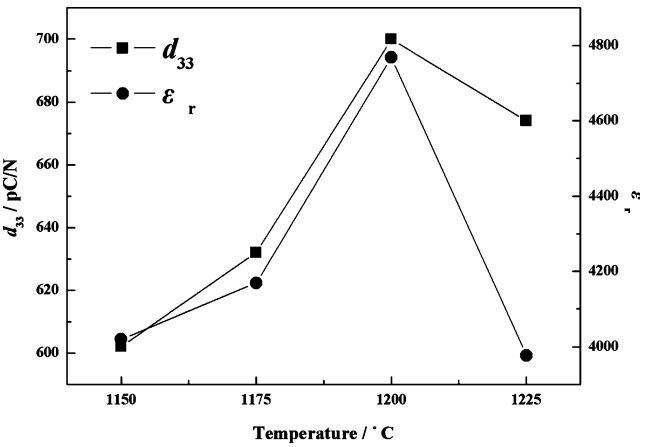


**Fig. 5** The piezoelectric constant $d_{33}$ and dielectric constant $\varepsilon_r$ of the specimens sintered at various temperatures

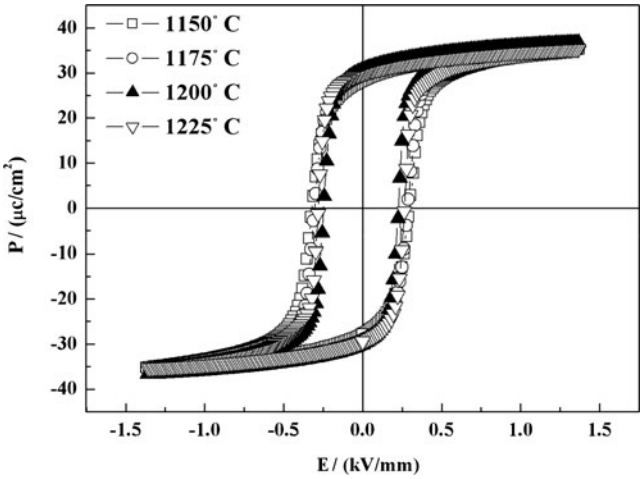


**Fig. 6** P − E hysteresis loops of PMN-0.345PT ceramics sintered at various temperatures

ferroelectric test system (TF Analyzer 2000, aixACCT, Germany).

## 3 Results and discussion

### 3.1 Microstructure of the PMN-0.345PT ceramics

Figure 2 illustrates the XRD patterns of the PMN-0.345PT ceramics sintered at various temperatures. The peaks of the specimens are sharp, and their full widths at half maximum are narrow, indicating the high crystallinity of all the samples. No second phase, except for a perovskite single phase, is observed at all sintering temperatures.

The microstructures of the sintered specimens were observed by SEM. The cross-sectional morphologies of the materials under various sintering temperatures are shown in Fig. 3. All specimens exhibit good density, and their cross-sections have no obvious delamination at the layer interfaces, suggesting the successful fabrication of the PMN-0.345PT piezoelectric ceramics by tape-casting. The grain size increases with increasing sintering temperature. Relatively uniform grains are noted in the sample sintered at 1150°C, although some porosity is likewise observed (Fig. 3(a)). The grains in the sample sintered at 1175°C are also uniform, but the number of pores is less (Fig. 3(b)). When the sintering temperature increases to 1200°C, large-sized pores are absent, whereas the grain size remains uniform. An average grain size of 4–5 μm (Fig. 3(c)) is measured by the linear intercept method. Transgranular fractures are detected when the sintering temperature increases to 1225°C (Fig. 3(d)). The appearance of transgranular fractures could be a result of overfiring.

### 3.2 The physical and electrical properties of PMN-0.345PT ceramics

Figure 4 illustrates the densities $\rho$ of the ceramics sintered at various temperatures. The bulk density $\rho$ of the ceramics is measured by the Archimedes method. As the sintering temperature is increased, the sample density increases rapidly before 1200°C, and reaches a peak of 7.61 g/cm$^3$ at 1200°C. The results are in agreement with the SEM observations. This phenomenon can be explained by the enhancement of diffusion, which is the driving force for densification, with the sintering temperature. However, the sample density decreases rapidly with the further increase of sintering temperature to 1225°C. As Fig. 3(d) shows that transgranular fractures and non-uniform grain size of the ceramic originate from overfiring. And the non-uniform grain size of the ceramic maybe lead to the lower density.

The $d_{33}$ and $\varepsilon_r$ of the specimens at various sintering temperatures are shown in Fig. 5. Tape-cast ceramics achieve a $d_{33}$ of 700 pC/N at 1200°C, whereas PMN-0.345PT piezoelectric ceramics prepared by the traditional process achieve a value of only 632 pC/N. Thus, the tape-casting process is useful for enhancing the properties of PMN-0.345PT piezoelectric ceramics. The peak value of $\varepsilon_r$ is $4.77\times10^3$ at 1200°C.

Figure 6 presents the P-E hysteresis of the PMN-0.345PT ceramics at various sintering temperatures after poling. All ceramics exhibit typical ferroelectric properties. The apparently saturated P–E loops have relatively high residual polarization $P_r$. $P_r$ and the coercive electric field are determined to be 30.68 μC/cm$^2$ and 0.35 kV/mm at 1200°C, respectively.

Table 1 shows the properties of the PMN-0.345PT piezoelectric ceramics fabricated via the two methods. Compared with the ceramics with the same compositions prepared by the traditional process, the tape-casting process enhanced the properties of the resulting

**Table 1** Properties of PMN-0.345PT piezoelectric ceramics fabricated by the tape-casting process and traditional solid-state reaction method

| Samples | $d_{33}$ (pC/N) | $k_p$ | $\varepsilon_r$ | tan$\delta$ | $P_r$ (μC/cm$^2$) |
|---|---|---|---|---|---|
| Solid-state reaction | 632 | 0.5914 | $3.63\times10^3$ | 0.014 | 29.09 |
| Tape-casting | 700 | 0.6050 | $4.77\times10^3$ | 0.014 | 30.68 |

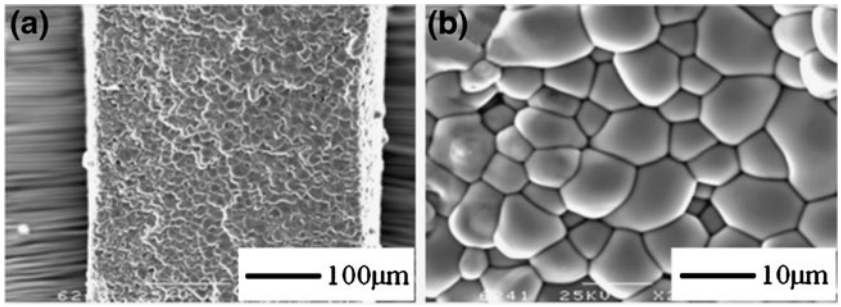


**Fig. 7** The microstructure of the cross-section of the fabricated FG actuator. (**a**) Low magnification and (**b**) high magnification

ceramics, as evidenced by the enhancement of $d_{33}$ from 632 to 700 pC/N.

### 3.3 Performance measurement of FG actuator

In the present study, four material compositions selected from the PMN-PT family are used as materials for the four layers in a new FG piezoelectric actuator. The high-strain layer (material A) has a $d_{33}$but small $\varepsilon_r$. In contrast, the low-strain layer (material D) has a small $d_{33}$ but a large $\varepsilon_r$. The four materials were laminated in the order of A − B − C − D. The $d_{33}$ and $\varepsilon_r$ of the four layers are listed in Table 2.

Figure 7 presents the microstructure of the FG actuator, which was observed at several positions in the thickness direction of a cross-section by SEM. No obvious difference is observed in the microstructures of the different layers.

The relationship between the displacement and voltage of the actuator was determined. A triangular wave was applied to the FG actuator with frequencies of 0.5, 1, 5, 10, and 20 Hz and AC electric fields with a driving voltage of 0–110 V (peak-to-peak). Displacement was measured by a laser displacement sensor (Keyence, LC-2440). The results are shown in Fig. 8. An increase in the driving voltage causes a gradual increase in the driving displacement of the free end of the actuator, and displacement increases in a linear manner. When the frequency applied to the FG actuator is 1 Hz and the driving voltage is 110 V, the driving displacement of the free end reaches 430.668 μm.

**Table 2** Piezoelectric constant $d_{33}$ and dielectric constant $\varepsilon_r$ of the four PMN-PT ceramics layers

| Samples | $d_{33}$ (pC/N) | $\varepsilon_r$ | tan$\delta$ |
|---|---|---|---|
| A $0.655Pb(Mg_{1/3}Nb_{2/3})O_3$-$0.345PbTiO_3$ | 700 | $4.77\times10^3$ | 0.014 |
| B $0.850Pb(Mg_{1/3}Nb_{2/3})O_3$-$0.150PbTiO_3$ | 260 | $3.63\times10^3$ | 0.30 |
| C $0.900Pb(Mg_{1/3}Nb_{2/3})O_3$-$0.100PbTiO_3$ | 106 | $1.29\times10^4$ | 0.70 |
| D $0.920Pb(Mg_{1/3}Nb_{2/3})O_3$-$0.080PbTiO_3$ | 65 | $1.69\times10^4$ | 0.71 |

## 4 Conclusions

$0.655Pb(Mg_{1/3}Nb_{2/3})O_3$-$0.345PbTiO_3$ piezoelectric ceramics were prepared by the tape-casting process. Delamination was not observed in the cross-sectional morphologies of the samples. The results indicate that tape-casting successfully yields PMN-0.345PT piezoelectric ceramics. The sintering temperature had a significant effect on the properties of the fabricated ceramics. The ceramics sintered at 1200°C exhibited outstanding properties, including $d_{33}$=700 pC/N, $\varepsilon_r=4.77\times10^3$, $k_p$=0.61, tan $\delta$=0.014, $P_r$=30.68 μC/cm$^2$. Compared with the ceramics with the same composition prepared by the traditional process, tape-casting enhanced the properties of the ceramics, resulting in an enhanced $d_{33}$ from 632 to 700 pC/N.

A new FG actuator was also successfully prepared. The driving displacement of its free end was 249.03 μm when the frequency signal applied to it is 0.5 Hz and the driving voltage is 110 V.

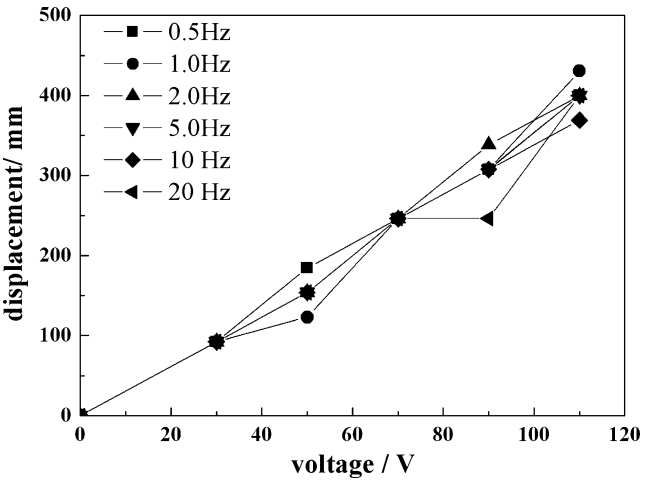


**Fig. 8** Displacement versus voltage of the fabricated FG actuator

**Acknowledgement** The present research was supported by the PCSIRT (IRT0968), the NSFC (90923029), the NSFC-NSF research (51161120326), the NSF of Jiangsu Province of China (BK2009020), the PNCET in University (NCET-10-0070), the NUAA Research Fund for Fundamental Research (NJ2010010, NZ2010001), the PAPD, the Aeronautical Science Fund (No. 2009ZF52058), Open Fund of State Key Lab of Digital Manufacturing Equipment and Technology of China (No. DMETKF2009002).

## References

1. A.J. Moulson, J.M. Herbert, *Electroceramics*, 2nd edn. (Wiley, Chichester, 2003)
2. K. Uchino, *Ferroelectric Devices*, 2nd edn. (Marcel Dekker, New York, 2000)
3. G.H. Haertling, Ferroelectric ceramics: history and technology. J. Am. Ceram. Soc. **82**, 797–818 (1999)
4. K.M. Rittenmyer, Electrostrictive ceramics for underwater transducer applications. J. Acoust. Soc. Am. **95**, 849–856 (1994)
5. L.E. Cross, S.J. Jang, R.E. Newnham, K. Uchino, Large electrostrictive effect in relaxor ferroelectrics. Ferroelectrics **23**, 187–191 (1980)
6. E.P. Smirnova, O.V. Rubinshtein, B.A. Isupov, Dielectric and electrostrictive properties of PMN-based complex perovskites. Ferroelectrics **143**, 263–270 (1993)
7. K. Kurihara, M. Kondo, High-strain piezoelectric ceramic and application on actuators. Ceram Intern **34**, 695–699 (2008)
8. H. Aburatani, S. Harada, K. Uchino, A. Furuta, Destruction mechanism in ceramic multilayer actuators. J. Appl. Phys. **33**, 3091–3094 (1994)
9. J. Qiu, J. Tani, D.J. Warkentin, T. Soga, Stress analysis of RAINBOW actuators and relief of stress by gradation of material composition. J. Japan. Soc. Appl. Electromagn. Mech. **7**, 185–192 (1999)
10. J. Tani, J. Qiu, T. Morita, Functionally gradient piezoelectric actuators. Trans. Mater. Res. Soc. **26**, 283–286 (2001)
11. J. Qiu, J. Tani, T. Morita, T. Ueno, T. Morita, H. Takahashi, H. Du, Fabrication and high durability of functionally graded piezoelectric bending actuators. Smart Mater. Struct. **12**, 115–121 (2003)
12. Y. Zeng, D.L. Jiang, P. Greil, Tape casting of aqueous $Al_2O_3$ slurries. J. Eur. Ceram. Soc. **20**, 1691–1697 (2000)
13. R.E. Mistler, E.R. Twiname, Tape casting: theory and practice. J. Am. Ceram. Soc. **37**, 43–48 (2000)
14. M.R. Gongora-Rubio, P. Espinoza-Vallejos, L. Sola-Laguna, J.J. Santiago-Aviles, Overview of low temperature cofired ceramics tape technology for meso-system technology (MsST). Sens Actuators-A **89**, 222–241 (2001)
15. S. Beaudet-Savignat, M. Chiron, C. Barthet, Tape casting of new electrolyte and anode materials for SOFCs operated at intermediate temperature. J. Eur. Ceram. Soc. **27**, 673–678 (2007)
16. H.Y. Dang, I.L. Burtrand, Processing of barium titanate tapes with different binders for MLCC applications-Part I: Optimization using design of experiments. J. Eur. Ceram. Soc. **24**, 739–752 (2004)
17. G. Besendorfer, A. Roosenw, Particle shape and size effects on anisotropic shrinkage in tape-cast ceramic layers. J. Am. Ceram. Soc. **91**, 2514–2520 (2008)
18. J.C. Beom, E.T. Park, J.M. Lee, Novel structure of ceramic tape for multilayer devices. J. Eur. Ceram. Soc. **29**, 451–456 (2009)
19. K. Okazaki, K. Nagata, Effects of grain size and porosity on electrical and optical properties of PLZT eeramics. J. Am. Ceram. Soc. **56**, 82–86 (1973)